Available online at www.sciencedirect.com

SCIENCE DIRECT®

Organic Electronics 5 (2004) 1–6

Organic Electronics

www.elsevier.com/locate/orgel

Exploring the polymorphism of crystalline pentacene

Raffaele Guido Della Valle [a],*, Aldo Brillante [a], Elisabetta Venuti [a],
Luca Farina [a], Alberto Girlando [b], Matteo Masino [b]

[a] *Dipartimento di Chimica Fisica e Inorganica, INSTM-UdR Bologna, Università di Bologna, Viale Risorgimento 4, I-40136 Bologna, Italy*

[b] *Dipartimento di Chimica, G.I.A.F. and INSTM-UdR Parma, Università di Parma, Parco Area delle Scienze, I-43100 Parma, Italy*

Received 25 June 2003; accepted 15 August 2003
Available online 9 April 2004

Abstract

Starting from each of the five complete X-ray structures published so far for crystalline pentacene, we have computed the structures of minimum potential energy, and obtained two local minima of the potential energy, i.e., two different "inherent structures" of mechanical equilibrium. This behavior, which has been found to be independent of the details of the potential model, indicates that there are at least two different single crystal polymorphs of pentacene. One of the two polymorphs corresponds to the structure originally determined by Campbell et al. [Acta Cryst. 14 (1961) 705]. The other polymorph corresponds to the structure found in all more recent measurements. The calculations predict significant differences between the corresponding Raman spectra of the lattice phonons, which we have checked experimentally, confirming the existence of two polymorphs. The correct identity of the samples, initially assigned only by matching experimental and calculated spectra, has been verified directly with X-ray diffraction measurements. Finally, we have obtained theoretical information on the global stability of the minima by systematically sampling the potential surface of crystalline pentacene, and found that the two polymorphs correspond to the two deepest minima. Further deep minima with layered structures, which might correspond to the thin film polymorphs found to grow on substrates, are also predicted.

PACS: 61.50.Ah; 81.30.Hd; 63.20.−e
Keywords: Crystal structures; Crystal modeling; Phase transitions; Phonon Raman spectra

---

1. Introduction

The reports about the extraordinary transport properties of pentacene [1], recognized as spurious, have now been retracted [2]. Nevertheless, pentacene remains one of the organic compounds with the highest electronic mobility [3]. The crystallographic investigations on pentacene have yielded five complete X-ray structures for single crystals [4–8]. Additional forms, whose unit cells have not yet been described, are found in thin films vapor grown on substrates [3,6,9–12]. Remarkably, this information was not sufficient to solve all doubts [3,5,6,13] about the existence of the various phases. In particular, the first X-ray structure of crystalline

---

* Corresponding author. Tel.: +39-51-2093710; fax: +39-51-2093690.
E-mail address: valle@aronte.fci.unibo.it (R.G. Della Valle).
URL: http://www.fci.unibo.it/~valle.

1566-1199/$ - see front matter © 2004 Elsevier B.V. All rights reserved.
doi:10.1016/j.orgel.2003.08.017

pentacene, reported by Campbell et al. [7,8] in the early 1960s, could not be reproduced by more recent studies [3–6].

We have dedicated considerable efforts to clarify this situation, using a combination of theoretical [14,15] and experimental [16–20] methods, and we can now conclusively show that the single crystal structure reported by Campbell et al. [7,8] is genuine and constitutes a distinct polymorph of pentacene (phase **C**). The structure reported by most other authors [3–6] is another polymorph (phase **H**). In this paper we focus on some aspects of our investigations on the pentacene polymorphs, including theoretical results [14,15], Raman spectra of the lattice phonons [16–18], and X-ray measurements [20]. Further information which may contribute to the understanding of the material, such as the spectra of the intramolecular modes, the optical absorption and reflectivity measurements, and an extended analysis of the effects of pressure and temperature, is available in the original papers [14–20].

2. Theoretical stability of the single crystal structures

As discussed in Section 1, we have first aimed to identify the genuinely different polymorphs among the various single crystal X-ray structures [4–8]. As a theoretical tool at this purpose, we have adopted the concept of "inherent structure", originally developed by Stillinger and Weber [21] to describe liquid and glassy states. This concept, which states that the "natural" or "inherent" structures that a system can exhibit correspond to the mechanically stable configurations at the *local minima* of the potential energy, provides a device to eliminate the "noise" due to the thermal expansion. Starting from a given configuration of the system, we follow a steepest descent minimization procedure to identify the structure at the local minimum of the potential energy. Different X-ray structures of the same thermodynamic phase, measured in different conditions of temperature or pressure, should all be situated in the attraction basin of the same local minimum, and should therefore converge toward identical inherent structures. Thus, the comparison of the inherent structures can be used to diagnose the identity, or lack of identity, of two phases. Binding energies and vibrational frequencies of the lattice, which probe the intermolecular interactions and thus depend directly on the relative arrangement of the molecules, may also be compared. Since the various comparisons can be hindered by small differences in the molecular geometries, it is preferable to use a unique geometry for all calculations. In all results presented in this paper, we use the ab initio geometry computed with a 6-31G(d) basis set in combination with an exchange-correlation functional B3LYP [22,23]. The intermolecular potential Φ is represented by an atom–atom Buckingham model [24], with Williams parameter set IV [25].

The five published X-ray structures of pentacene [4–8] all belong to the triclinic space group $P\bar{1}(C_i^1)$,

Table 1
Calculated data for the six deepest minima

N		Energy	a	b	c	α	β	γ	Space group	Z
1	Calc.	−41.073	5.980	7.441	15.070	97.90	98.49	93.49	$P\bar{1}$ (C_i^1)	2
	Expt. [8]		6.06	7.90	14.88	96.74	100.54	94.20	$P\bar{1}$ (C_i^1)	2
2	Calc.	−40.916	6.053	7.434	14.973	78.73	84.56	85.91	$P\bar{1}$ (C_i^1)	2
	Expt. [6]		6.266	7.775	14.530	76.47	87.68	84.68	$P\bar{1}$ (C_i^1)	2
3	Calc.	−40.612	6.032	7.424	14.885	87.16	82.92	86.66	$P\bar{1}$ (C_i^1)	2
4	Calc.	−39.980	3.595	6.146	15.177	96.42	93.29	95.65	$P\bar{1}$ (C_i^1)	1
5	Calc.	−39.948	31.331	3.599	12.219	90.00	106.03	90.00	$C2/c$ (C_{2h}^6)	4
6	Calc.	−39.840	15.079	3.597	12.266	90.00	95.31	90.00	$P2_1/c$ (C_{2h}^5)	2

For each minimum, we report its energy rank $N = 1$–6, molar potential energy (kcal/mol), lattice parameters (axes a, b, c in Å, and angles α, β, γ in degrees), space group, and number Z of molecules in the unit cell. For polymorphs **C** ($N = 1$) and **H** ($N = 2$), we also report the corresponding experimental data [6,8] at room temperature. Transformations to reduced cells [29] have been enforced where necessary.

with two independent molecules per unit cell, located on inversion centers. Starting separately from each structure [4–8], we have replaced the experimental molecular geometries with the ab initio one, and then minimized the total potential energy of the crystal Φ with respect to lattice parameters, molecular positions and orientations. We have thus found two distinct minima [15,17], indicated in Table 1 with $N = 1$ and 2. The minimum $N = 1$ is reached only when starting from the structure of Campbell et al. [7,8], while all other structures [4–6] converge to minimum $N = 2$. According to our previous discussion, these two minima correspond to different polymorphs, which we have labeled **C** and **H**, respectively. This conclusion does not depend on the details of the calculations, since we have also tried other geometries [15] and other potential models [17], always obtaining the same relationships among the minima. As shown in Table 1, the structures of minimum energy remain quite close to the corresponding experimental structures [6–8], which are satisfactorily reproduced.

3. Detecting the polymorphs with Raman and X-ray experiments

Once theoretically shown that structures **C** and **H** are distinct phases of pentacene, we were left with the experimental problem of obtaining, identifying and studying samples of the two polymorphs. To simplify the discussion, we anticipate here the conclusion that we have identified vapor grown single crystals of pentacene with two different morphologies, actually corresponding to polymorphs **C** and **H**. The experimental evidence of the existence of two distinct single crystal phases is compelling and has been obtained by comparing both the X-ray diffraction patterns (the unit cell structure) and the Raman spectra of lattice phonons (the unit cell dynamics) of the polymorphs [16,20].

The method of crystal growth, from solution or vapor, does not appears to be the determining factor for obtaining either structure. Most of the commercial products that we have tested (Koch & Light, Fluka purum, Aldrich) are mainly constituted by phase **H** with phase **C** as physical impurity [16]. This finding is consistent with the observation [3,6] that single crystals of pentacene normally assume the **H** structure, as shown by most X-ray experiments [4–6]. Sublimation in a hydrogen stream also usually yields dark blue platelets belonging to phase **H**. Tiny blue microcrystals belonging to polymorph **C** can instead be obtained by fast sublimation at about 500 K in inert atmosphere (nitrogen or argon) at pressures from 2.5 to 10 kPa.

We used the Raman spectra of the lattice phonons to discriminate between the two phases, since the calculations predicted [15,17] large differences between their Raman phonon spectra. Typical Raman spectra for the two morphologies are shown in Fig. 1. We only report the region 20–180 cm^{-1}, where all lattice phonons are visible. The evident differences between the spectra are already sufficient to show that they belong to distinct phases. As discussed elsewhere [15–17], the assignment of the spectra to polymorphs **C** and **H** was initially based on the comparison between experimental [18] and calculated [15] Raman frequencies of the lattice modes. This information is reported in Table 2. It can be noticed that the calculated frequencies reproduce quite well the characteristic frequency patterns of the two polymorphs. Such a spectroscopic assignment, although quite reliable, cannot provide absolute certainty. We thus have checked the identity of the samples by recording their X-ray powder diffraction diagrams, and verified that the two different

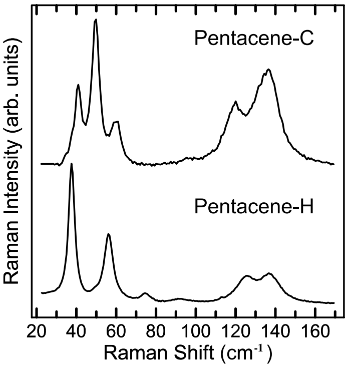

Fig. 1. Raman spectra of pentacene polymorphs **C** and **H** at 300 K.

Table 2
Raman frequencies (cm^{-1}) of the lattice modes of pentacene

Polymorph **C**		Polymorph **H**	
Expt.	Calc.	Expt.	Calc.
49.4	46.7	44.9	33.5
54.9	57.2	65.5	64.1
66.9	72.5	84.3	76.9
99.8	115.0	99.1	110.2
140.6	155.8	144.1	157.9
147.5	164.8	149.5	164.2

The A_g frequencies calculated [15] at the inherent structures for phases **C** and **H** are compared to the experimental [18] Raman frequencies at 79 K.

single crystal morphologies can also be identified directly with X-ray diffraction experiments [20]. Indeed, these yield two distinct structures, matching the published experimental data of both forms **C** [7,8] and **H** [4–6].

4. Effects of pressure and temperature

Since Raman spectroscopy proved so effective in the identification of the polymorphs of pentacene, we decided to use it also to investigate about the effects of pressure and temperature on the vibrational properties and the relative stability of the phases **C** and **H**. Raman experiments as a function of pressure [19,20] have thus revealed that polymorph **C** transforms irreversibly into the denser polymorph **H**, with a sluggish phase transition starting around 0.2 GPa. Spectra taken by heating or cooling over a wide range of temperatures (4.2–400 K), did not reveal instead any phase transition [18]. The remarkable thermal stability of phases **C** and **H** is confirmed by the observation that the pressure induced phase transition is insensitive to temperature effects [19,20], because thermal annealing under pressure does not affect the transition rate.

5. Global stability of the minima

Once shown that two polymorphs exist and correspond to two *local* minima of the potential, it becomes desirable to investigate on their *global* stability and on the possible occurrence of further polymorphs. This was achieved by performing a systematic sampling of the potential energy surface [14], i.e., by predicting the possible crystal structures [26,27]. A Quasi Monte Carlo sampling scheme, based on a low-discrepancy Sobol' sequence [28], was used to generate 3500 different triclinic structures with two independent molecules for the unit cell. Each of these configurations was used as the starting point of a steepest descent energy minimization procedure. After discarding all configurations which failed to converge to stable bound states (≈40%), we analyzed the structures at the potential minima to identify their space group, a step which occasionally involved cell halving or doubling to obtain a conventional reduced cell [29]. Once identified all structures encountered more than once, we were left with about 340 distinct minima, with a surprising large variety of structural arrangements. As discussed elsewhere [14], we have probably identified a large part of the accessible minima. While increasing the coverage of the search space, in fact, we encounter a saturation plateau where to find new minima becomes progressively more difficult, because new configurations tend to fall more and more frequently onto previously encountered minima.

As an example of the kind of structures that we have encountered, we have drawn in Fig. 2 the structures of the six deepest minima, all occurring in a narrow energy range (≈0.2 kcal/mol). Molar potential energy, space group and crystallographic parameters of these six minima are reported in Table 1. The two deepest minima, indicated in Table 1 with rank $N = 1$ and 2, coincide with the previously identified phases **C** and **H**. The experimental lattice parameters [6–8] of the polymorphs **C** and **H**, also reported in Table 1 are reproduced fairly well by the computed parameters of the two corresponding minima.

Since several other deep minima are predicted, further polymorphs are expected to exist. It should be recalled that all proposed additional polymorphs [3,6,10–12] appear to grow in conditions where the interaction with a substrate might contribute to their stability. The deep minima presented in Fig. 2 and Table 1 present "layered" structures in which the molecules remain approximately aligned and lie

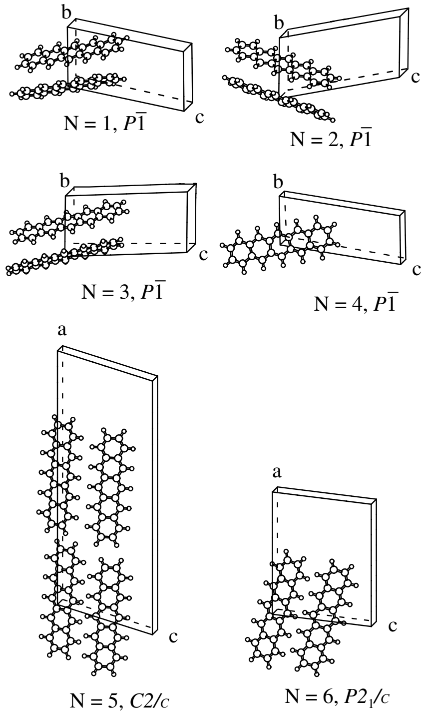

N = 1, $P\bar{1}$ N = 2, $P\bar{1}$ N = 3, $P\bar{1}$ N = 4, $P\bar{1}$ N = 5, $C2/c$ N = 6, $P2_1/c$

Fig. 2. Calculated structures of the six deepest minima. The shortest cell axis is approximately perpendicular to the plane of the page. Minima are labeled by their energy rank N (as indicated in Table 1) and their space group. Molecular graphics were obtained with MOLSCRIPT [30].

on planes with very short inter-plane distances (minor cell axis ≈3.6 Å), an arrangement which may indeed enhance the stabilizing interaction with the substrate. Since most deep minima differ for the space group and for the number of molecules in the unit cell, they should be easily discriminated with spectroscopic methods.

6. Discussion and conclusions

We have reached conclusive experimental and theoretical evidence that the single crystal structures of pentacene reported by Campbell et al. [7,8] and by Holmes et al. [3–6] are both reproducible and constitute two distinct phases of pentacene, which we have labeled polymorphs **C** and **H**, respectively. The polymorphs have been discriminated with Raman phonon spectra [16–18], and X-ray [20] experiments. The calculations [14] indicate that polymorphs **C** and **H** corresponds to the two deepest minima of the potential energy of the system.

The calculations also predict further deep minima with layered structures. These structures might correspond to the thin films polymorphs grown on substrates [3,9–12], which are usually experimentally identified by the value $d(0\,0\,1)$ of the distance between the ab crystallographic planes, which constitutes the largest repeat unit in the lattice. Since a more complete structural determination is not always possible, this distance is the main, and often the only, criterion used to identified the various phases. Mattheus et al. have recently [3] used this criterion to show that four different polymorphs, identified by $d(0\,0\,1)$ spacing of 14.1, 14.4, 15.0 and 15.4 Å, can be obtained in thin film form, depending on growth conditions. Measurements as a function of temperature indicate that the 14.1 and 14.4 Å phases are thermally the most stable ones. The 15.0 and 15.4 Å phases are less stable and can be transformed into the 14.1 and 14.4 Å phases, respectively, by raising the temperature or by exposition to solvents. Part of the unit cell parameters of the various phases could be determined by X-ray or electron diffraction. Although incomplete, this information was sufficient for a comparison with the published single crystal structures [3–8]. It has thus been clearly shown [3] that the 14.1 Å phase correspond to polymorph **H**, the form normally assumed by single crystals of pentacene [3–6]. Since the single crystal polymorph **C** is thermally stable and has a $d(0\,0\,1)$ spacing of 14.5 Å, it would be very tempting to identify it with the 14.4 Å thin film phase. However, this possibility does not seem to be supported by the available structural data [3].

Finally, it should be clearly noticed that our experiments and calculations all refer to the single crystal structures of pentacene. We expect significant differences with the vapor grown films, as also shown by the variations in the structural measurements [3,9–12] on thin film samples grown on different substrates. These differences might be crucial in comparing data. Raman spectra on the thin film forms, and further X-ray measurements on both the single crystal and thin film forms, will certainly help in clarifying these issues.

References

[1] J.H. Schön, Ch. Kloc, B. Batlogg, Science 288 (2000) 2338.

[2] Z. Bao, B. Batlogg, S. Berg, A. Dodabalapur, R.C. Haddon, H. Hwang, Ch. Kloc, H. Meng, J.H. Schön, Science 298 (2002) 961.

[3] C.C. Mattheus, A.B. Dros, J. Baas, G.T. Oostergetel, A. Meetsma, J.L. de Boer, T.T.M. Palstra, Synth. Met. 138 (2003) 475.

[4] T. Siegrist, Ch. Kloc, J.H. Schön, B. Batlogg, R.C. Haddon, S. Berg, G.A. Thomas, Angew. Chem. Int. Ed. Engl. 40 (2001) 1732.

[5] D. Holmes, S. Kumaraswamy, A.J. Matzger, K.P. Vollhardt, Chem. Eur. J. 5 (1999) 3399.

[6] C.C. Mattheus, A.B. Dros, J. Baas, A. Meetsma, J.L. de Boer, T.T.M. Palstra, Acta Cryst. C 57 (2001) 939.

[7] R.B. Campbell, J.M. Roberston, J. Trotter, Acta Cryst. 14 (1961) 705.

[8] R.B. Campbell, J.M. Roberston, J. Trotter, Acta Cryst. 15 (1962) 289.

[9] C.D. Dimitrakopoulos, A.R. Brown, A. Pomp, J. Appl. Phys. 80 (1996) 2501.

[10] I.P.M. Bouchoms, W.A. Schoonveld, J. Vrijmoeth, T.M. Klapwijk, Synth. Met. 104 (1999) 175.

[11] D.J. Gundlach, T.N. Jackson, D.G. Schlom, S.F. Nelson, Appl. Phys. Lett. 74 (1999) 3302.

[12] S. Lukas, G. Witte, Ch. Wöll, Phys. Rev. Lett. 88 (2002) 028301.

[13] C.C. Mattheus, G.A. de Wijs, R.A. de Groot, T.T.M. Palstra, J. Am. Chem. Soc. 125 (2003) 6323.

[14] R.G. Della Valle, E. Venuti, A. Brillante, A. Girlando, J. Chem. Phys. 118 (2003) 807.

[15] E. Venuti, R.G. Della Valle, A. Brillante, M. Masino, A. Girlando, J. Am. Chem. Soc. 124 (2002) 2128.

[16] A. Brillante, R.G. Della Valle, L. Farina, A. Girlando, M. Masino, E. Venuti, Chem. Phys. Lett. 357 (2002) 32.

[17] M. Masino, A. Girlando, R.G. Della Valle, E. Venuti, L. Farina, A. Brillante, Mat. Res. Soc. Symp. Proc. 725 (2002) 149.

[18] R.G. Della Valle, E. Venuti, L. Farina, A. Brillante, M. Masino, A. Girlando, J. Phys. Chem. B 108 (2004) 1822.

[19] L. Farina, K. Syassen, A. Brillante, R.G. Della Valle, E. Venuti, N. Karl, High Pressure Res. 23 (2003) 349.

[20] L. Farina, A. Brillante, R.G. Della Valle, E. Venuti, M. Amboage, K. Syassen, Chem. Phys. Lett. 375 (2003) 490.

[21] F.H. Stillinger, T.A. Weber, Phys. Rev. A 25 (1982) 978.

[22] M.J. Frisch et al., Gaussian 98, Revision A.7, Gaussian Inc., Pittsburgh, PA, 1998.

[23] C. Lee, W. Yang, R.G. Parr, Phys. Rev. B 37 (1988) 785.

[24] A.J. Pertsin, A.I. Kitaigorodsky, The Atom-Atom Potential Method, Springer-Verlag, Berlin, 1987.

[25] D.E. Williams, J. Chem. Phys. 47 (1967) 4680.

[26] J.P.M. Lommerse et al., Acta Cryst. B 56 (2000) 697.

[27] W.D.S. Motherwell et al., Acta Cryst. B 58 (2002) 647.

[28] W.H. Press, S.A. Teukolsky, W.T. Vetterling, B.P. Flannery, Numerical Recipes in Fortran, Cambridge University Press, Cambridge, 1992.

[29] Y. Le Page, J. Appl. Cryst. 21 (1988) 983.

[30] P.J. Kraulis, J. Appl. Cryst. 24 (1991) 946. http://www.avatar.se/molscript/.